Melting, superheating and freezing behaviour of indium interpreted using a nucleation-and-growth model

2001 J. Phys.: Condens. Matter 13 11443

(http://iopscience.iop.org/0953-8984/13/50/304)

INSTITUTE OF PHYSICS PUBLISHING JOURNAL OF PHYSICS: CONDENSED MATTER

J. Phys.: Condens. Matter **13** (2001) 11443–11452 PII: S0953-8984(01)28222-8

Melting, superheating and freezing behaviour of indium interpreted using a nucleation-and-growth model

J Zhong, Z H Jin and K Lu[1]

Shenyang National Laboratory for Materials Science, Institute of Metal Research, Chinese Academy of Sciences, Shenyang 110016, People's Republic of China

E-mail: kelu@imr.ac.cn (K Lu)

Received 22 August 2001
Published 30 November 2001
Online at stacks.iop.org/JPhysCM/13/11443

Abstract

The traditional phenomenological asymmetry between melting and freezing has been studied by varying the crystal nucleation behaviour during freezing and the liquid nucleation behaviour during melting. The existence of a series of freezing peaks, whose shapes resemble normal melting peaks of bulk In, of In melt with pre-existing crystal nuclei has been demonstrated experimentally by means of accurate differential scanning calorimetry (DSC). A superheating peak has been investigated by using DSC for In nanoparticles embedded in an Al matrix. A phenomenological kinetic symmetry between melting and freezing has been demonstrated using DSC curves, which suggests that the melting and superheating behaviour of metal can be interpreted in terms of non-nucleation, heterogeneous nucleation and homogeneous nucleation models, respectively.

1. Introduction

Although melting, as a mysterious phenomenon in nature, has attracted much attention for a long time, a general theory for this phase transformation has not been established. Lindemann [1] first formulated a criterion for crystal–liquid transition: that melting is a vibrational instability released when the root mean square amplitude of vibration reaches a critical fraction of the interatomic distance. Cotterill [2] related melting to dislocation generation, whereas Górecki [3] emphasized vacancies as a crucial factor during melting. In a comprehensive survey, Boyer [4] concluded that lattice shear instability is the precipitating feature for melting. Since the superheating phenomenon was first observed in experiments [5–8], a succession of stability limits for the crystalline state have been proposed in terms of different models, although a consensus theory has not been reached yet. Fecht and Johnson [9]

[1] Author to whom any correspondence should be addressed.

0953-8984/01/5011443+10$30.00

first pointed to an entropy catastrophe as the ultimate stability limit for the superheated crystals. Tallon [10] suggested that for crystalline superheating a succession of catastrophes occur in the sequence elastic compressibility, elastic rigidity, isochoric (equal volumes for crystal and liquid) and, finally, entropic points.

Recent research results showed that the nucleation-and-growth model, as an established model for solidification, might reasonably account for the melting and superheating behaviour of metal crystals. Lu and Li [11] found that a homogeneous nucleation catastrophe would arrive before any of the other catastrophes put in an appearance as a kinetic stability limit for superheated crystals. This degree of kinetic superheating (about $0.20T_0$, where T_0 is thermodynamic equilibrium melting point for bulk metals) predicted on the basis of homogeneous nucleation is close to that ($0.22T_0$) of ideal bulk metal as simulated by means of molecular dynamics (MD) for the element Al [12]. Furthermore, Zhang *et al* [13] recently observed a superheating phenomenon in Pb metal thin films and thermodynamic analysis indicated that such superheating might result from suppression of growth of the molten droplets.

However, an unambiguous viewpoint on melting and superheating in terms of the nucleation-and-growth model has not been reached yet. This reflects the argument on the phenomenological kinetic symmetry or asymmetry between melting and freezing. Conventionally, a fundamental phenomenological kinetic asymmetry is observed between melting and freezing: upon heating, a crystal melts when the temperature approaches T_0; while on cooling, a liquid crystallizes usually some degrees below T_0. This phenomenon is frequently referred to as phenomenological kinetic asymmetry between melting and freezing [14], which is supposed to originate from the fact that melting initiates at surfaces or interfaces where nucleation for the liquid phase is unnecessary or the nucleation energy barrier is negligible, while freezing of a melt has to overcome a substantial energy barrier for crystal nucleation. (It must be noted that the concept of symmetry/asymmetry between melting and freezing treated here is only on a phenomenological basis, as discussed later.) Recently, Chattopadhyay and Goswami [15] highlighted this phenomenological kinetic asymmetry in the melting and freezing of embedded Bi particles, whereas Cahn and Johnson [16] stressed an important phenomenological kinetic symmetry between melting and freezing when metastable superheating was convincingly observed for solid elements of Ag [5] and Ar [8].

Differential scanning calorimetry (DSC) is a reliable experimental method for studying crystal–liquid transformation. As the difference in specific heats of the liquid and the solid for metals is often less than or equal to 10%, the heat-flow DSC signal y per unit mass of specimen can be simplified as [17]

$$y = a\frac{\mathrm{d}T}{\mathrm{d}t} + \Delta H_0 \frac{\mathrm{d}f(T,t)}{\mathrm{d}t}. \tag{1}$$

The parameter a is related to the mass and specific heats of the specimen and the standard. T is temperature, t is time, $\mathrm{d}T/\mathrm{d}t$ is the scanning rate and $f(T,t)$ is the fraction of new phase. ΔH_0 is the enthalpy change, which is positive for melting and negative for freezing.

In this work, melting and freezing processes of a bulk In sample and In nanoparticles embedded in an Al matrix were studied by using DSC. A viewpoint regarding melting and superheating of metals as processes of nucleation and growth has been supported by DSC curves. It is suggested that interfaces play an important role during melting and superheating.

2. Experimental details

A pure bulk In sample with a purity of 99.999% was provided by Perkin-Elmer Company. An alloy ingot with a nominal composition of Al–10 wt% In was prepared by arc melting

of 99.999% pure Al and 99.999% pure In in water-cooled copper crucibles under an Ar atmosphere. In/Al ribbons with widths of 2–3 mm and thicknesses of 30–40 μm were obtained by using melt spinning under an Ar atmosphere.

The experiments were performed on a Perkin-Elmer differential scanning calorimeter (DSC, Pyris 1). The power precision of the instrument is 0.2 μW. The temperature and energy accuracies of Pyris 1 DSC were calibrated by means of pure In at a scanning rate of 10 K min^{-1}. The pure bulk In sample of 6.160 mg was sealed in an Al pan and monitored in flowing Ar (99.999%) atmosphere. Five scanning rates of 0.1, 1.0, 1.5, 2.0 and 3.0 K min^{-1} were used. Just the one sample was used repeatedly to study the melting and freezing processes at different scanning rates in order to eliminate effects of sample size and weight on DSC curves. The mass of the In/Al ribbon sample sealed in the Al pan was 31.790 mg and the measurement was conducted at a scanning rate of 10 K min^{-1} under a flowing Ar atmosphere.

3. Results and discussion

In figure 1(a) curves A and B are the DSC signals of normal melting and freezing for pure bulk In at 1 K min^{-1}. The conspicuous above-mentioned phenomenological kinetic asymmetry can be seen between the positions and peak shapes of the melting peak and the freezing peak. The onset temperature (429.7 K) of the melting peak is close to its equilibrium melting point T_0 (429.8 K); while the onset temperature of the freezing peak is about 1.8 K below T_0. The peak temperature in the cooling curve is even higher than the onset temperature. That indicates that the exothermal rate during freezing is so large that it can elevate the sample temperature at a cooling rate of 1 K min^{-1}. The slope of the right-hand side of the freezing peak, obviously negative, is much steeper than that of the left-hand side of the melting peak. The peak height of the melting peak is 1.9430 mW mg^{-1}, while that of the freezing peak is -6.0589 mW mg^{-1}. In expression (1), a can be seen as a constant for a given specimen and standard. When $\mathrm{d}T/\mathrm{d}t$ is given, the variation of the DSC signal y depends on $f(T, t)$. For melting of bulk metallic solid, it is nucleation-free or the degree of heterogeneous nucleation is so small to be negligible; for freezing of bulk metallic liquid, a heterogeneous nucleation process is unavoidable. This difference in intrinsic transition mechanism influences the temperature and the transition rate, i.e., $f(T, t)$, which results in the discrepancies between the DSC curves for melting and freezing.

In order to investigate the freezing behaviour of a melt with pre-existing crystal nuclei, we heated the In solid sample above T_0 and then cooled it down when the solid was partially melted. In figure 1, curves C and D are typical partial melting and freezing signals for partially melted In solid. From these measurements, one may see that

(i) the peak temperature for the freezing process with pre-existing crystal nuclei is only about 0.3 K below T_0, which is much smaller than the value for the normal freezing process ($\sim$1.8 K);
(ii) the shape of the freezing peak with pre-existing crystal nuclei is very similar (but upside-down) to that of the normal melting peak (see the inset of figure 1(a)).

In order to compare these peaks, the peak height h (mW mg^{-1}), freezing enthalpy change ΔH_{pf} (J g^{-1}) and slope s (mW mg^{-1} s^{-1}) for the freezing peak with pre-existing crystal nuclei, as indicated in the inset of figure 1(a), are determined.

By cooling the liquid–solid mixture at different stages (in the partial melting process), one may obtain different amounts of pre-existing crystals and corresponding partial freezing DSC peaks as shown in figure 1(b). With variation of the portion of liquid in the mixture, the freezing peak height and the enthalpy change vary accordingly. Figure 2 shows the variation

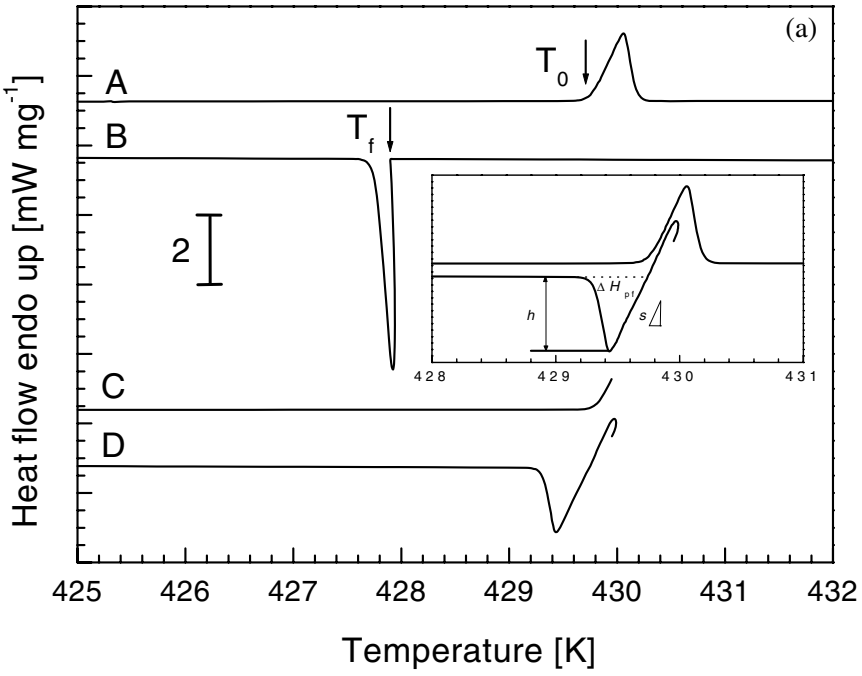

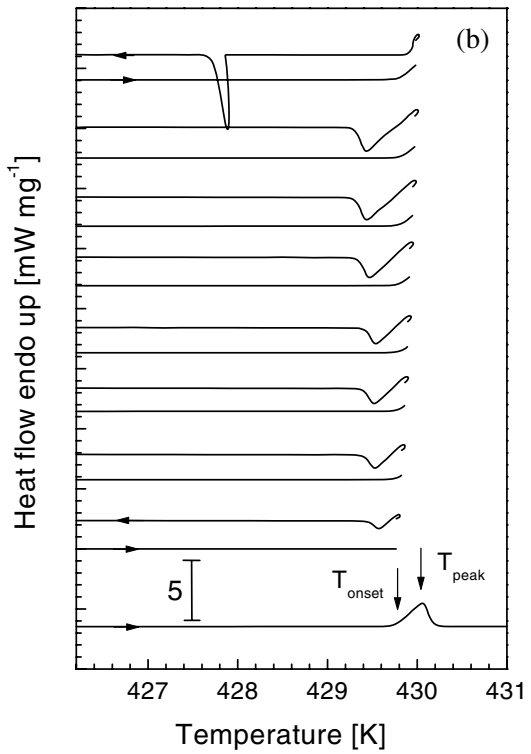

Figure 1. (a) DSC curves for pure bulk In at 1 K min^{-1}: A, normal melting; B, normal freezing; C, partial melting; and D, freezing of the liquid–solid mixture. (b) A series of partial freezing DSC peaks with different amounts of pre-existing crystal at 1 K min^{-1}.

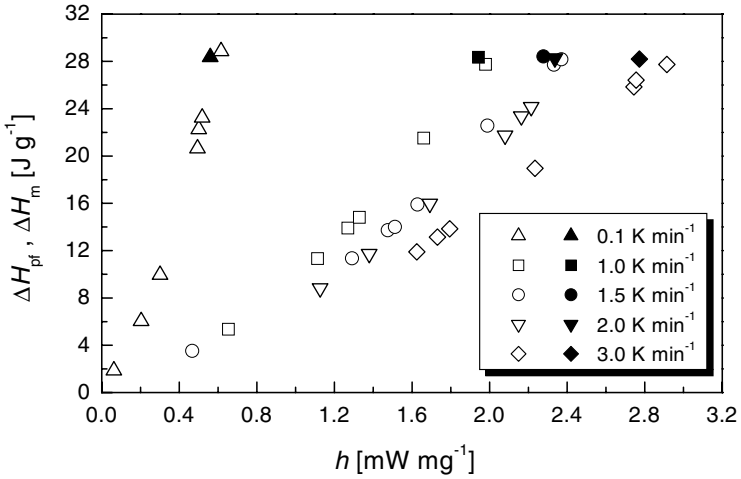

Figure 2. The variation of the freezing enthalpy change (ΔH_{pf}) with the peak height (h) for In melt with pre-existing crystal at different scanning rates, compared to that for normal melting peaks. As indicated, the solid square, circle, upward-pointing triangle, downward-pointing triangle and diamond are for normal melting, and the open symbols are for freezing of the partially melted In. Only absolute values of h, ΔH_{pf} and ΔH_m (melting enthalpy change) are employed for comparison.

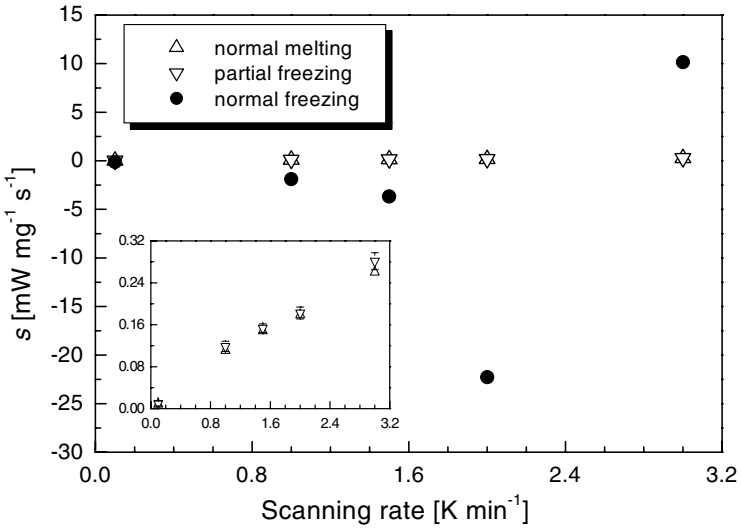

Figure 3. The left-hand side slope values (s) of normal melting peaks and right-hand side slope values (s) of partial freezing peaks and normal freezing peaks at different scanning rates.

of the freezing enthalpy change ΔH_{pf} with the peak height h, compared with that of the normal melting. It is clear that at various cooling rates, with increase of the peak height (h), the ΔH_{pf} values increase gradually and approach the normal melting enthalpy change ΔH_m (28.45 J g^{-1}). Here only absolute values of h, ΔH_{pf} and ΔH_m are employed for comparison.

Figure 3 shows left-hand side slope values (s) of normal melting peaks and right-hand side slope values (s) of partial freezing peaks and normal freezing peaks at different scanning

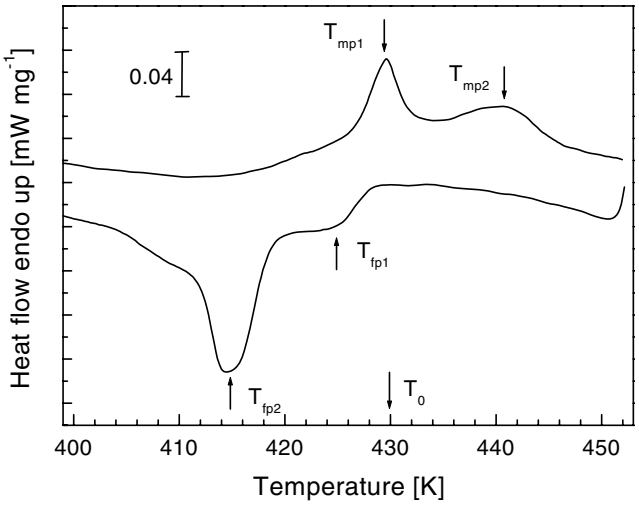

Figure 4. DSC curves for melting and freezing at 10 K min^{-1} for In nanoparticles embedded in an Al matrix.

rates. For normal freezing, the slope value shows a large variation at different cooling rates. At and below a cooling rate of 2 K min^{-1}, the slope value is negative and reduces gradually with increasing cooling rate. At a cooling rate of 3 K min^{-1}, the slope value becomes positive. This change of the slope value during normal freezing can be attributed to competition between the exothermal rate resulting from heterogeneous nucleation and the programmed cooling condition. The slope of the normal freezing peak will reach an infinite value at a certain cooling rate between 2 and 3 K min^{-1}. The slope value of normal melting peaks and that of partial freezing peaks overlap, even on a much smaller y-coordinate scale as seen in the inset of figure 3. In fact, as in figure 1(b), the slope values of partial freezing peaks are almost unchanged for different h-values at one cooling rate, which indicates that the freezing velocity is independent of the amount of the proportion of pre-existing crystals.

From the above results, one can see that the characteristics of DSC peaks of partial freezing differ substantially from those for normal freezing, but are analogous to those for normal melting. This indicates that the transition temperature and the transition rate, i.e., $f(T, t)$ in equation (1), of partial freezing have been changed a lot compared to those for normal freezing. That is to say, the freezing behaviour of pure In has been altered by leaving a proportion of the solid as a pre-existing nucleus, in which the freezing process is dominated by the growth process rather than heterogeneous nucleation.

As for the melt-spun In/Al ribbons, the uniformly distributed In particles, most of which are single crystal, show a cube–cube orientation relationship with the Al matrix, which can be described as $\{111\}_{\mathrm{Al}} \parallel \{111\}_{\mathrm{In}}$ and $\langle 110\rangle_{\mathrm{Al}} \parallel \langle 110\rangle_{\mathrm{In}}$. Among those single-crystal In particles, some are truncated octahedral, bounded by $\{111\}_{\mathrm{Al}}$ and $\{100\}_{\mathrm{Al}}$ facets. Semi-coherent interfaces between In and Al are constructed (for structural details, see [18–20]). The average particle size of embedded In in this sample is about 25 nm as established by transmission electron microscopy and x-ray diffraction measurements.

The calorimetric curves for In nanoparticles embedded in the Al matrix are shown in figure 4. Two endothermal peaks are found in the heating curve. The first one's peak temperature is around 429.6 K, which results from those random particles distributed at grain boundaries of Al or inside Al grains. The second one's peak temperature is 440.7 K,

about 11 K above T_0; i.e., there is a superheating of In, which results from these faceted single-crystal In nanoparticles. *In situ* high-resolution electron microscopy experiments [21] investigated heterogeneous nucleation of melting occurring at the interfaces {100} for faceted In nanoparticles, which contributed to the observed superheating phenomena. So, by changing the interfacial structure of In/Al, the melting point of embedded In nanoparticles has been enhanced. Melting behaviour of superheated In nanoparticles is characterized by heterogeneous nucleation rather than non-nucleation or negligible heterogeneous nucleation. Two exothermal peaks, one with a supercooling of 2–10 K and another with a supercooling of 10–25 K, in the cooling curve for the In/Al sample are investigated. The higher-temperature freezing peak results from those bigger particles which are nucleated by catalytic trace impurities. The lower-temperature freezing peak can be ascribed to those smaller faceted In nanoparticles which nucleate at the $\{111\}_{\mathrm{Al}}$ facets [22, 23]. The supercooling phenomenon indicates that heterogeneous nucleation of In particles in this sample is necessary during freezing.

The above experimental results on melting of In crystals embedded in an Al matrix prove that when a coherent (or semi-coherent) In/Al interface is constructed, In can be substantially superheated. This means that when the surface melting is effectively suppressed, melting nucleation—either heterogeneous, at the interfaces or other defects, or homogeneous, in the inner part of the crystal—is necessary and will shift the melting process above T_0, i.e. a superheating occurs. On the basis of the classic homogeneous nucleation analysis by Lu and Li [11], the heterogeneous nucleation process for the melting of superheated crystals can be analysed. The heterogeneous nucleation rate of a liquid can be expressed as

$$I_{\mathrm{heter}} = I_0 \exp\left(-\frac{\Delta G^*(T) f(\theta)}{kT}\right) \exp\left(-\frac{Q}{kT}\right) \tag{2}$$

where

$$f(\theta) = (2 - 3\cos(\theta) + \cos^3(\theta))/4$$
$$\cos(\theta) = (\sigma_{ms} - \sigma_{ml})/\sigma_{sl}$$
$$\Delta G^*(T) = 16\pi\sigma_{sl}^3/3(\Delta G_v + \Delta E)^2$$
$$\Delta G_v = \Delta H_0(T_0 - T)/T_0.$$

σ_{ms}, σ_{sl} and σ_{ml} are respectively the interface energies of matrix–solid, solid–liquid, matrix–liquid interfaces. ΔH_0 denotes the fusion enthalpy change. ΔE is the change in strain energy density (per unit volume) resulting from the volume change upon melting. I_0 is a prefactor related to the vibration frequency of the atoms and the surface area of the liquid nucleus, Q is the activation energy for atomic diffusion across the solid–liquid interface and k is Boltzmann's constant. Owing to the critical nucleation energy, $\Delta G^*(T) f(\theta)$ is always smaller than $\Delta G^*(T)$; the degree of superheating derived from equation (2) is always smaller than that from the homogeneous nucleation, and is dependent upon the θ-values. In other words, the superheating due to the heterogeneous nucleation of melting may vary over a range between T_0 and $1.20T_0$ (from homogeneous nucleation theory), which can account for the different degrees of superheating observed in experiments [18–21, 27–32].

Figure 5 shows a schematic overview illustrating a phenomenological kinetic symmetry between melting and freezing processes in terms of the nucleation-and-growth model by means of DSC curves. Three melting–freezing pairs are compared separately—corresponding to non-nucleation, heterogeneous nucleation and homogeneous nucleation. Normally, non-nucleation melting and heterogeneous nucleation freezing are mostly observed in experiments, which leads to the argument of phenomenological kinetic asymmetry between melting and freezing. Freezing processes with homogeneous nucleation are visible in certain cases when

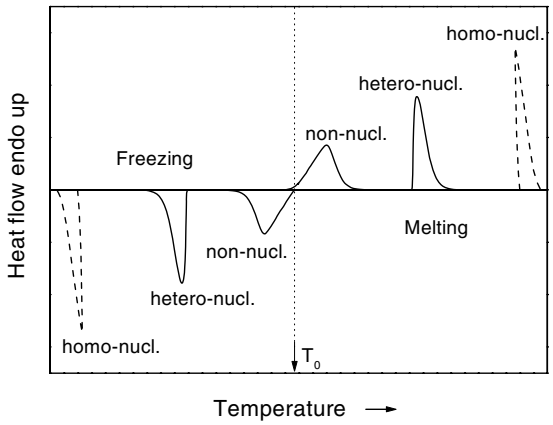

Figure 5. A schematic diagram showing the phenomenological kinetic symmetry between melting and freezing exhibited by DSC curves.

the heterogeneous nucleation is suppressed. Melting processes with homogeneous nucleation are investigated in MD simulations [12]. The non-nucleation freezing process for partially melted In solid and heterogeneous nucleation melting for embedded In nanoparticles are clearly demonstrated in the present work, which contributes to an overall phenomenological kinetic symmetry between melting and freezing.

The roles played by various interfaces during melting and freezing processes with heterogeneous nucleation can be seen in figure 6. For heterogeneous nucleation melting, as shown in figure 6(a), $\cos(\theta) = (\sigma_{ms} - \sigma_{ml})/\sigma_{sl}$; for heterogeneous nucleation freezing, as shown in figure 6(b), $\cos(\theta') = (\sigma_{ml} - \sigma_{ms})/\sigma_{sl}$. If the values of σ_{ms}, σ_{ml} and σ_{sl} are supposed to remain the same for melting and freezing, then $\theta' = 180^\circ - \theta$. That is to say, under the assumption of constant interface energies for a given system, if the solid and the matrix exist first, melting of the solid must form a liquid nucleus corresponding to the contact angle θ; if the liquid and the matrix exist first, freezing of the liquid must form a solid nucleus corresponding to the contact angle $180^\circ - \theta$.

It must be mentioned that only when $(\sigma_{ml} - \sigma_{sl}) < \sigma_{ms} < (\sigma_{ml} + \sigma_{sl})$ is the notion of heterogeneous nucleation applicable for melting. When $\sigma_{ms} < (\sigma_{ml} - \sigma_{sl})$ or melting is initiated at the centre of a single crystal, homogeneous nucleation is operative. When $\sigma_{ms} > (\sigma_{ml} + \sigma_{sl})$, the notion of nucleation is inappropriate for melting, because there is no θ-value for the condition $\sigma_{ms} = \sigma_{sl}\cos(\theta) + \sigma_{ml}$, which implies that melting can be initiated from the surface or interface spontaneously at T_0 (such as in normal melting of bulk solid) or even below T_0 (such as in the melting point depression of low-dimension materials) [24–26]. By changing the relations among σ_{ms}, σ_{ml} and σ_{sl}, different degrees of superheating in crystal can be obtained.

From the above analysis, two ways of keeping a metal in the solid state above its T_0 can be considered. One is to enable heterogeneous or homogeneous nucleation to occur unavoidably during melting, such as in superheating of embedded nanoparticles of In [18–21], Pb [27–31], Ag [32]; another way is to suppress the growth process of a molten phase, such as in the superheating of a constrained Pb film in Al [13]. *In situ* high-resolution electron microscopy observation of In particles embedded in an Al matrix showed that a liquid phase of In nucleated at a {100} facet, which assumed two configurations alternately before reaching the next {100} facet; this stage was the rate-controlling process [21]. This result implied that the processes

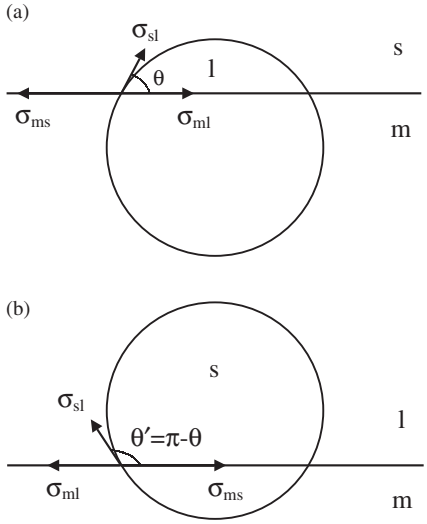

Figure 6. An illustration of melting (a) and freezing (b) with heterogeneous nucleation, showing the relationship of the contact angles when the values of σ_{ms}, σ_{ml} and σ_{sl} are the same for melting and freezing.

of nucleation and growth occurring during melting might be suppressed in sequence.

The symmetry between melting and freezing is discussed here only on a phenomenological basis; it does not mean complete mirror symmetry between these two processes in the transition temperature and the transition rate. For a given element or system, ΔE is very different during melting and freezing. For most metals except for Bi, Ga, Ge, Si, the effect of ΔE is significant due to a volume expansion during melting, whereas it can be negligible due to a volume constraint during freezing. The activation energy of atomic diffusion, Q, during melting is obviously much smaller than that during freezing due to the higher phase transition temperature of melting. These two factors will render it impossible for melting and freezing to be two mirror-symmetric processes when there is superheating and supercooling. In fact, using the universal order parameter model of the crystal–melt transition derived from the microscopic density functional theory, Iwamatsu [33] predicted spinodals and an asymmetry between the degree of superheating and that of supercooling.

Recent MD simulation results indicated that the accumulation and coalescence of internal local lattice instabilities serves as the primary mechanism for homogeneous melt nucleation inside a surface-free Lennard-Jones crystal [34] and suggested that the vibrational and elastic lattice instability criteria as well as the homogeneous nucleation theory combine to determine the superheating limit. However, the mechanism for heterogeneous nucleation during melting is not yet clear. More experimental and MD simulation studies need to be carried out in order to establish the effects of heterogeneous nucleation and growth on superheating of metals.

4. Conclusions

A series of partial freezing peaks for partially melted In were obtained in DSC measurements at different scanning rates; nucleation and supercooling were avoided and a peak shape similar to that for normal melting was seen. A melting peak for superheated In nanoparticles was obtained by DSC, which indicated that heterogeneous nucleation was involved in the phase

transition. The experimental results contribute to an argument of phenomenological kinetic symmetry between melting and freezing, which implies that the nucleation-and-growth model may be applicable for understanding melting and superheating behaviour of metals. Analysis results show that the interface energies σ_{ms}, σ_{ml} and σ_{sl} play an important role in dominating melting and superheating processes of a metallic solid.

Acknowledgments

We would like to gratefully acknowledge financial support from the National Science Foundation of China (grants Nos 59841004, 59801011 and 59931030), the Ministry of Science and Technology of China (grant No 1999064505) and the Max-Planck Society of Germany.

References

[1] Lindemann F A 1910 *Z. Phys.* **11** 609
[2] Cotterill R M J 1980 *J. Cryst. Growth* **48** 582
[3] Górecki T 1974 *Z. Metallk.* **65** 426
Górecki T 1976 *Z. Metallk.* **67** 269
[4] Boyer L L 1985 *Phase Transitions* **5** 1
[5] Daeges J, Gleiter H and Perepezko J H 1986 *Phys. Lett.* A **119** 79
[6] Uhlmann D R 1980 *J. Non-Cryst. Solids* **41** 347
[7] Jung J and Franck J P 1987 *Japan. J. Appl. Phys. Suppl.* 3 **26** 399
[8] Rossouw C J and Donnelly S E 1985 *Phys. Rev. Lett.* **55** 2960
[9] Fecht H J and Johnson W L 1988 *Nature* **334** 50
[10] Tallon J L 1989 *Nature* **342** 658
[11] Lu K and Li Y 1998 *Phys. Rev. Lett.* **80** 4474
[12] Jin Z H and Lu K 1998 *Phil. Mag. Lett.* **78** 29
[13] Zhang L, Jin Z H, Zhang L H, Sui M L and Lu K 2000 *Phys. Rev. Lett.* **85** 1484
[14] Christian J W 1965 *The Theory of Transformation in Metals and Alloys* (Oxford: Pergamon) p 587
[15] Chattopadhyay K and Goswami R 1997 *Prog. Mater. Sci.* **42** 287
[16] Cahn R W and Johnson W L 1986 *J. Mater. Res.* **1** 724
[17] O'Reilly K A Q and Cantor B 1996 *Proc. R. Soc.* A **452** 2141
[18] Saka H, Nishikawa Y and Imura T 1988 *Phil. Mag.* A **57** 895
[19] Zhang D L and Cantor B 1991 *Acta Metall. Mater.* **39** 1595
[20] Sheng H W, Ren G, Peng L M, Hu Z Q and Lu K 1997 *J. Mater. Res.* **12** 119
[21] Sasaki K and Saka H 1991 *Phil. Mag.* A **63** 1207
[22] Zhang D L and Cantor B 1990 *Phil. Mag.* A **62** 557
[23] Goswami R, Chattopadhyay K, Kim W T and Cantor B 1992 *Metall. Trans.* A **23** 3207
[24] Takagi M 1954 *J. Phys. Soc. Japan* **9** 359
[25] Buffat Ph and Borel J-P 1976 *Phys. Rev.* A **13** 2287
[26] Goldstein A N, Echer C M and Alivisatos A P 1992 *Science* **256** 1425
[27] Gråbæk L, Bohr J, Johnson E, Sarholt-Kristensen A and Andersen H H 1990 *Phys. Rev. Lett.* **64** 934
[28] Goswami R and Chattopadhyay K 1993 *Phil. Mag. Lett.* **68** 215
[29] Goswami R and Chattopadhyay K 1995 *Acta Metall. Mater.* **43** 2837
[30] Andersen H H and Johnson E 1995 *Nucl. Instrum. Methods Phys. Res.* B **106** 480
[31] Sheng H W, Ren G, Peng L M, Hu Z Q and Lu K 1996 *Phil. Mag. Lett.* **73** 179
[32] Zhong J, Zhang L H, Jin Z H, Sui M L and Lu K 2001 *Acta Mater.* **49** 2897
[33] Iwamatsu M 1999 *J. Phys.: Condens. Matter* **11** L1
[34] Jin Z H, Gumbsch P, Lu K and Ma E 2001 *Phys. Rev. Lett.* **87** 055703